

## Effect of dopant concentration on photocatalytic activity of TiO<sub>2</sub> film doped by Mn non-uniformly

Kaijian Zhang<sup>1,3</sup>, Wei Xu<sup>2</sup>, Xinjun Li<sup>2\*</sup>, Shaojian Zheng<sup>2</sup>, Gang Xu<sup>2</sup>

<sup>1</sup> *Economy, Industry and Business Management College,  
Chongqing University,  
400044 Chongqing, People Republic of China*

<sup>2</sup> *Institute Guangzhou Institute of Energy Conversion,  
Chinese Academy of Sciences,  
510640 Guangzhou, People Republic of China*

<sup>3</sup> *Institute Panzhihua Iron & Steel Research Institute,  
Panzhihua I & S Ltd. Co,  
Panzhihua 617000, People Republic of China*

Received 22 October 2005; accepted 31 January 2006

**Abstract:** The thin films of TiO<sub>2</sub> doped by Mn non-uniformly were prepared by sol-gel method under process control. In our preceding study, we investigated in detail, the effect of doping mode on the photocatalytic activity of TiO<sub>2</sub> films showing that Mn non-uniform doping can greatly enhance the activity. In this study we looked at the effect of doping concentration on the photocatalytic activity of the TiO<sub>2</sub> films. In this paper, the thin films were characterized by UV-vis spectrophotometer and electrochemical workstation. The activity of the photocatalyst was also evaluated by photocatalytic degradation rate of aqueous methyl orange under UV radiation. The results illustrate that the TiO<sub>2</sub> thin film doped by Mn non-uniformly at the optimal dopant concentration (0.7 at %) is of the highest activity, and on the contrary, the activity of those doped uniformly is decreased. As a comparison, in 80 min, the degradation rate of methyl orange is 62 %, 12 % and 34 % for Mn non-uniform doping film (0.7 at %), the uniform doping film (0.7 at %) and pure titanium dioxide film, respectively. We have seen that, for the doping and the pure TiO<sub>2</sub> films, the stronger signals of open circuit potential and transient photocurrent, the better photocatalytic activity. We also discuss the effect of dopant concentration on the photocatalytic activity of the TiO<sub>2</sub> films in terms of effective separation of the photon-generated carriers in the semiconductor.

© Versita Warsaw and Springer-Verlag Berlin Heidelberg. All rights reserved.

*Keywords:* TiO<sub>2</sub>, Mn, dopant concentration, non-uniform

---

\* E-mail: lixj@ms.giec.ac.cn

## 1 Introduction

TiO<sub>2</sub> photocatalysis has been extensively investigated with its oxidation being applied to environmental remediation processes [1–3]. Although the application of the material has been baffled by its low photo quantum efficiency of photocatalytic process, a series of photocatalytic techniques have been formed in recent years in order to enhance efficiency of photocatalytic process, such as noble metal loading, semiconductor composite, metal ion doping, etc. [4–6]. The 3d-transition metal doped anatase TiO<sub>2</sub> is the usual modification method. Choi et al. [7] have studied completely the doping effect of twenty-one kinds of transitional metal ions on nano-crystalline TiO<sub>2</sub>. They have demonstrated that the photocatalytic activity is greatly affected by the doping concentration of metal ions, and that each different ion has an optimal concentration, respectively.

In our previous paper [8], we investigated completely the effect of doping mode on the photocatalytic activity of TiO<sub>2</sub> films and explained the definition of uniform doping and non-uniform doping. We have also proven the existence of PN junction in the non-uniform doping TiO<sub>2</sub> films. Our experimental results illustrated that Mn non-uniform doping can evidently enhance the photocatalytic activity of TiO<sub>2</sub> thin film, and that Mn uniform doping decrease the activity.

For the photocatalytic activity of TiO<sub>2</sub> films being affected by the dopant concentration greatly, we will investigate, in detail, the effect of dopant concentration of Mn on photocatalytic activity of the TiO<sub>2</sub> films and will discuss the mechanism of the films affected by dopant concentration in terms of the characteristics of semiconductor.

## 2 Experimental

### 2.1 Preparation of substrate

Soda lime glass (200mm×34mm×2mm) pre-coated with a SiO<sub>2</sub> layer were used as the substrates for the thin films. To prevent the thermal diffusion of the sodium ions from the glass to TiO<sub>2</sub> films, a SiO<sub>2</sub> layer was pre-coated on the SL glass by the sol–gel method [9, 10]. Precursor solutions for SiO<sub>2</sub> thin films were prepared as below: Tetraethylorthosilicate (TEOS) (104 ml) was dissolved in an absolute ethanol solution (160 ml). While stirring, an additional hydrochloric acid (2 M, 26 ml) was added drop-wise to the above TEOS precursor. Thereafter the mixture was stirred for 1 hour, and then the mixture was aged for 24 h, resulting in the SiO<sub>2</sub> sol. The SiO<sub>2</sub> films formed on soda-lime glass were prepared from the above SiO<sub>2</sub> sol solution by dipping-withdrawing in an ambient atmosphere with a withdrawal speed of 4 mms<sup>-1</sup>. The substrates coated with SiO<sub>2</sub> gel films were heat-treated in air at a rate of 2 °C min<sup>-1</sup> up to 500 °C and were left to stay in the furnace at the highest temperature for about 1 h.

## 2.2 Preparation of Mn-doped and pure TiO<sub>2</sub> films

TiO<sub>2</sub>-sol: The sol was prepared by the following method [11]: 68 ml of Tetra-butyl-ortho-titanate and 16.5 ml of diethanolamine were dissolved in 210 ml absolute ethanol, and then the mixture was stirred vigorously for 1 hour (Solution A). While stirring, the mixture of 3.6 ml of water and 100 ml of absolute ethanol (Solution B) was added dropwise into the Solution A. The resulting alkoxide solution was left in the dark for 24 hours to form the TiO<sub>2</sub>-sol.

Mn/TiO<sub>2</sub>-sol: The preparation of Mn/TiO<sub>2</sub>-sol was similar to that of TiO<sub>2</sub>-sol; the only difference was that various amounts of Mn(NO<sub>3</sub>)<sub>2</sub> (Analytical Reagent) were added into 3.6 ml of H<sub>2</sub>O to make various concentrations of sol when Solution B was made. Each different concentration of Mn/TiO<sub>2</sub> sol (atomic ratio: 0.2 at %, 0.5 at %, 0.7 at %, 1.0 at %, 1.5 at %) was designated as MT<sub>x</sub> (x=0.2, 0.5, 0.7, 1.0, 1.5).

Samples of the doped or pure TiO<sub>2</sub> films formed on the soda lime glass (SLG) substrates with a SiO<sub>2</sub> layer were prepared from the TiO<sub>2</sub> sol or Mn/TiO<sub>2</sub> sol by the following steps:

- (1) Dipping–withdrawing at a speed of 2 mm·s<sup>-1</sup>;
- (2) Drying at 100 °C for 10 minutes;
- (3) Heating to 500 °C at the heating rate of 2 °C·s<sup>-1</sup>;
- (4) Keeping at 500 °C for 1 hour, and then cooling.

The films of TiO<sub>2</sub> in different doping modes described as Fig. 1 were prepared by repeating the above steps.

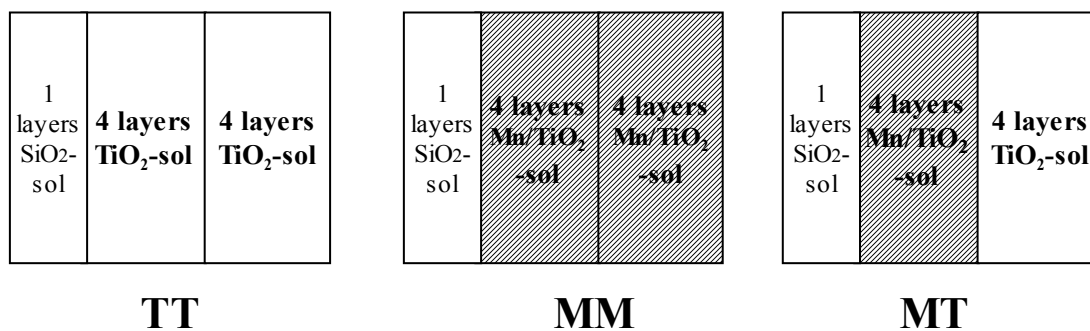


Fig. 1 The doping mode of TiO<sub>2</sub>.

## 2.3 Characterization

The thickness of TiO<sub>2</sub> films was measured by scanning electron microscopy (SEM; type JSM-5600LV) with an accelerating voltage of 25 kV. The TiO<sub>2</sub> films, determined by X-ray diffraction (XRD) using a diffract-meter (type D/MAX-.A) with Cu K $\alpha$  radiation, which accelerating voltage and the applied current were 30 kV and 30mA respectively, were in the form of anatase, according with reference [11]. XPS (X-ray photoelectron spectroscopy) spectra was acquired with an energy spectrometer (type PHI-5800) with a

Mg  $K_{\alpha}$  X-ray source operated at 15keV and 18mA. Each binding energy was referenced to the  $C_{1s}$  at 284.6 eV. Spectral analyses of  $TiO_2$  films were performed by a U-3010 UV-visible spectrophotometer, and the baseline was based on a piece of SLG with one  $SiO_2$  layer.

## 2.4 Electrochemistry experiments

In our experiments, the properties of the photocatalyst films were analyzed by means of electrochemistry with CHI660 electrochemical station.

### 2.4.1 Preparation of film electrode

The photocatalyst film electrode (20mm×20mm) was prepared with the method of section 2.1 (no  $SiO_2$  layer), after the ITO conductive glass was washed in the base solution and by ultrasonic vibrations.

### 2.4.2 Test of electrochemistry

Electrochemistry tests were performed in a three electrode system made of quartz cells linked to a CHI660 electrochemical station.  $TiO_2$ /ITO electrode was served as the working electrode (WE), a platinum sheet (20mm×20mm) and the saturation calomel electrode (SCE) were served as the counter electrode (CE) and the reference electrode, respectively. The electrolyte was 0.5 mol/L  $Na_2SO_4$  aqueous solution which was prepared by analytical reagents and distilled water. The lamp-house of the photo electrochemical test was a tungsten lamp (5W,  $\lambda_p=365$  nm). All tests were carried out at room temperature.

## 2.5 Photocatalytic activity test

The reactor was a glass cylinder ( $\Phi=70$  mm,  $H=240$  mm), in which five pieces of glass with photocatalyst film were settled tightly near to the container inside the wall. Then, 400 ml of aqueous methyl-orange (10 mg/L in reverse osmosis-treated water,  $pH=5.9$ ) was added into the cylinder, and the solution was aerated for 30 minutes before the experiment began in order to reach the surface absorption equilibrium of the  $TiO_2$  films. A high-pressure mercury lamp (125W  $\lambda_p=365$ nm) was preheated for 30 minutes and placed in the reactor center as a light-house. The reactor was immersed in a thermostatic bath in order to obtain a constant temperature, and the solution was stirred by bubbling with air during irradiation. The solution was sampled every 20 min. The concentration of aqueous methyl orange was determined by scanning the absorbance of the sample within the scope of 200-600 nm with a U-3010 UV-VIS spectrophotometer.

### 3 Results

#### 3.1 SEM observation and XPS analysis

The thickness of the films was measured by Scanning Electron Microscopy (SEM) after the cross-sections were sprayed with carbon film in a vacuum plating instrument. A typical SEM micrograph of cross-section of the TiO<sub>2</sub> film is shown in Fig. 2. The thickness of the TiO<sub>2</sub> film together with a layer SiO<sub>2</sub> is about 350 nm. The XPS could not detect manganese, since the amount of incorporated manganese is too low to be directly detected by the equipment. The fitting curve of O<sub>1s</sub> from XPS at the 100 nm depth of the Mn uniformly doping TiO<sub>2</sub> (MM1.5) thin film is shown in Fig. 3, there are only two fitting peaks of O<sub>1s</sub>, 530.6 eV and 529.6 eV, respectively, each of which may be from the oxygen in the O-Mn and O-Ti. Mn ion exists as Mn<sup>4+</sup> after Mn-doped TiO<sub>2</sub> are treated at 500 °C [13].

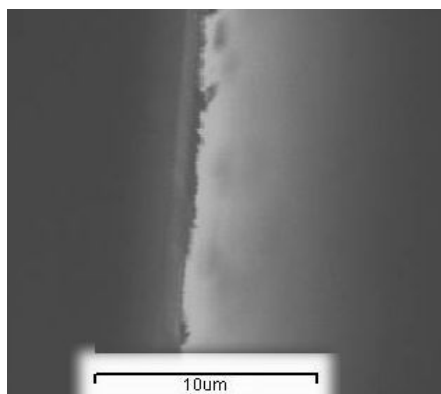


**Fig. 2** SEM micrograph of cross-section of the TiO<sub>2</sub> film together with a layer SiO<sub>2</sub>.

#### 3.2 Photooxidation activity

The activity of the photocatalyst was analyzed on the basis of photocatalytic reactions of aqueous methyl-orange. In 80 minutes, the degradation rate of aqueous methyl orange was 62 % for Mn non-uniformly doped film (0.7 at %), 12 % for the uniformly doped film (0.7 at %) and 34 % for pure titanium dioxide film, respectively. Fig. 4 shows the comparison of activities of TiO<sub>2</sub> films doped non-uniformly (MT) and uniformly (MM) by Mn at the doping concentration of 0.7 at %, with that of pure TiO<sub>2</sub> films (TT). Although the photocatalytic activity of MM films was evidently worse than that of TT, the activity of MT films was higher than that of TT.

Figure 5 presents the degradation rates of methyl orange degradation as a function of the dopant concentration of Mn in both MT mode and MM mode. For the MT mode, the activity increases with the Mn addition, maximizes at 0.7 at %, and then decreases with the more Mn addition. For the MM mode, the activity was worse than pure TiO<sub>2</sub> films, and the photocatalytic activity decrease gradually with the Mn addition increasing.

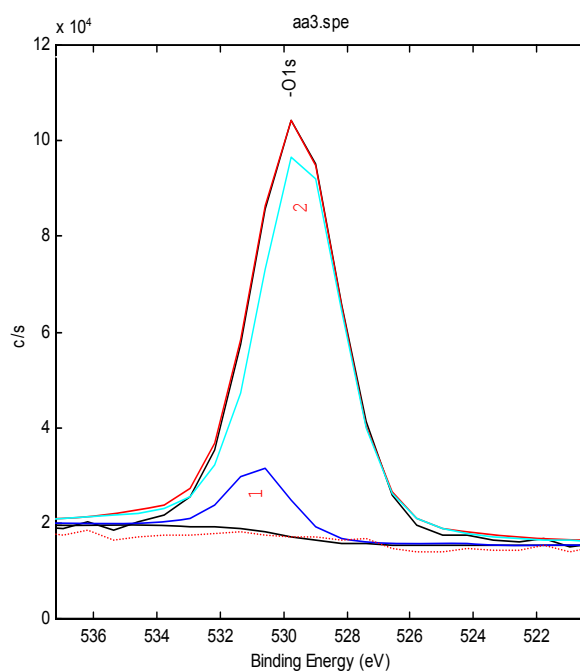


**Fig. 3** The fitted O<sub>1s</sub> XPS of the film in 100 nm (peak1: O-Mn, peak 2: O-Ti).

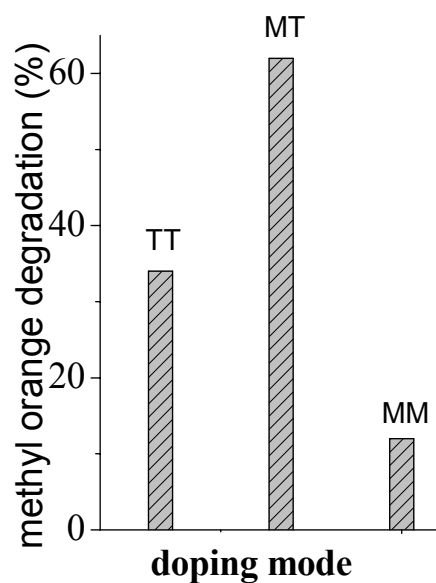


**Fig. 4** The curves of the degradation rate of aqueous methyl orange in 80 min at different doping mode.

### 3.3 Electrochemical properties

Open circuit potential reflects electric charge transferred onto the surface of semiconductor, and the transient photo-current reflects the conductance and number of free current carriers in the semiconductor. Fig. 6 and 7 show the variation of the open circuit potential and transient photo-current of the MT film electrodes with different dopant concentration,

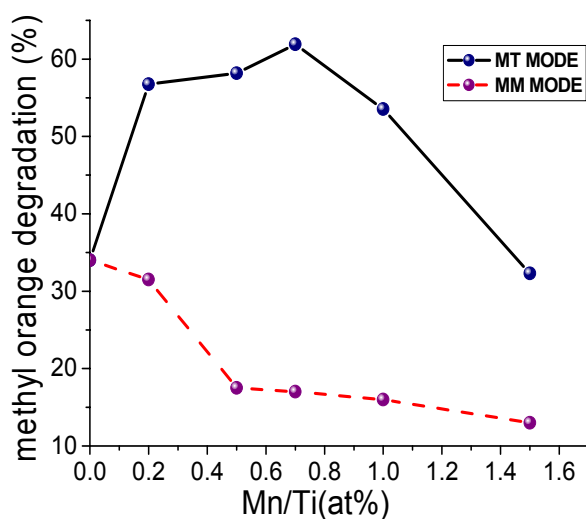


**Fig. 5** The curves of relation between degradation rate of aqueous methyl orange and Mn dopant concentration in MT mode.

respectively. The signal intensity of open circuit potential and the transient photo-current was enhanced gradually with the increase of Mn doping concentration, maximized at 0.7 at % , and then the more doping Mn in the films, the weaker signal. When the dopant concentration reached 1.5 at % , the signals was weaker than pure  $\text{TiO}_2$ .

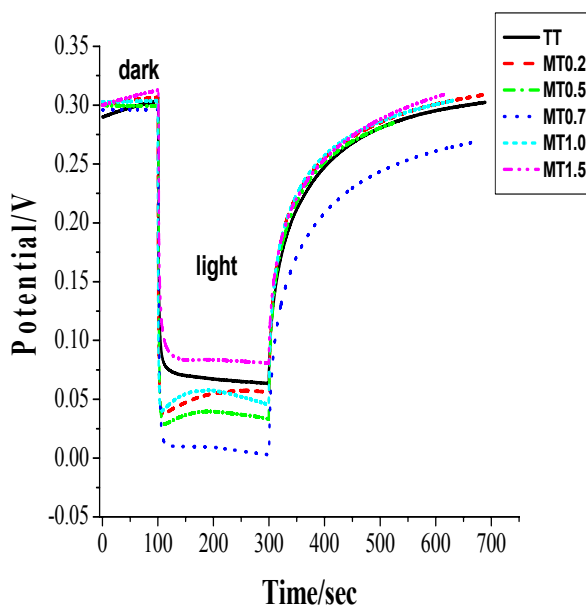


**Fig. 6** The open circuit potential of the Mn/ $\text{TiO}_2$  film electrodes under various dopant concentration vs time.

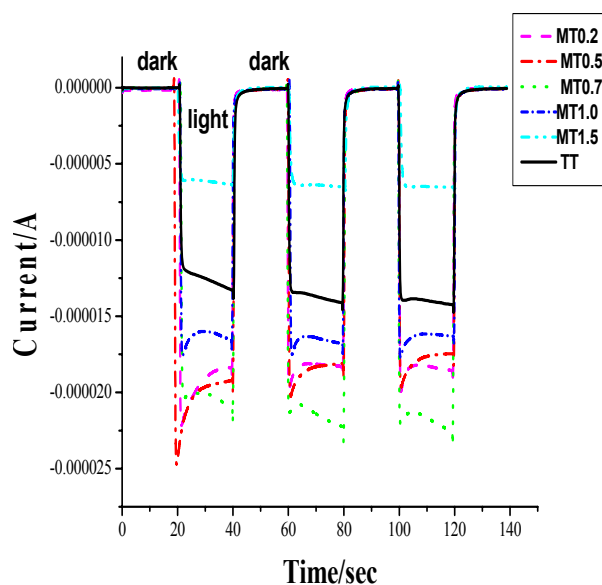


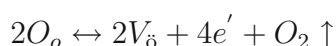
**Fig. 7** The amperometric current of the Mn/TiO<sub>2</sub> film electrodes under various doping concentration vs time.

### 3.4 UV-vis absorbency spectra

Fig. 8 shows the UV-Vis transmittance comparison of the TiO<sub>2</sub> films doped by Mn with different doping (MM and MT) modes at 0.7 at % dopant concentration with the pure one. It can be seen that the absorption edge of MM film is similar to that of the pure one, whereas, the absorption edge of MT film shows “red shift”. Fig. 9 shows the UV-Vis transmittance of the TiO<sub>2</sub> films doped by Mn with different dopant concentration. The absorption edges of the doped TiO<sub>2</sub> with 0.2, 0.5 0.7 and 1.0 at % dopant concentration have demonstrated “red shift”, except that with 1.5 at % dopant concentration. The “red shift” tendency of the doped TiO<sub>2</sub> varied with the dopant concentration is similar to that of the open circuit potential (see Fig. 6) and the transient photo-current (see Fig. 7). This phenomenon implies that the absorption of the doped TiO<sub>2</sub> would have some relation with the separation of photo generated carriers.

## 4 Discussion

Pure titania is a kind of non-stoichiometric compound of anion vacancies, and the chemistry formula is TiO<sub>2-x</sub> with the reaction formula of the defect as follows [14]:



where  $O_o$  is the oxygen atom on the perfect site of crystal lattice,  $V_{\bar{O}}$  is positively charged vacancy (with two positive charges) on O site and  $e'$  is quasi-free electron. Positively charged vacancy (relative to perfect lattice) on O site did bound two positive charges being equalized by quasi-free electron because of the escape  $O_2$ , and pure titanium dioxide is n-type semiconductor for the presence of oxygen atom vacancies.



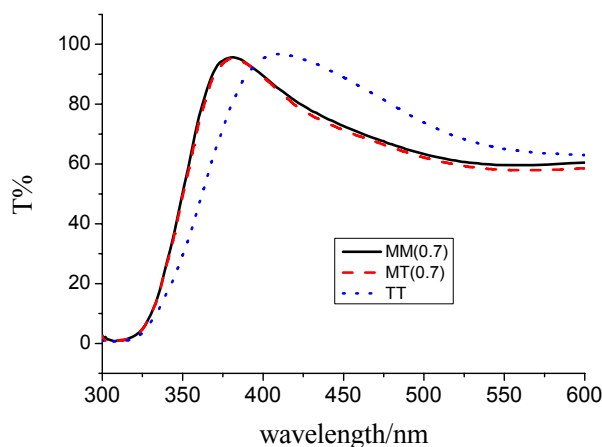


**Fig. 8** The UV-Vis transmittance comparison of the TiO<sub>2</sub> films doped by Mn with different doping (MM and MT) modes at 0.7 at % dopant concentration with the pure one.

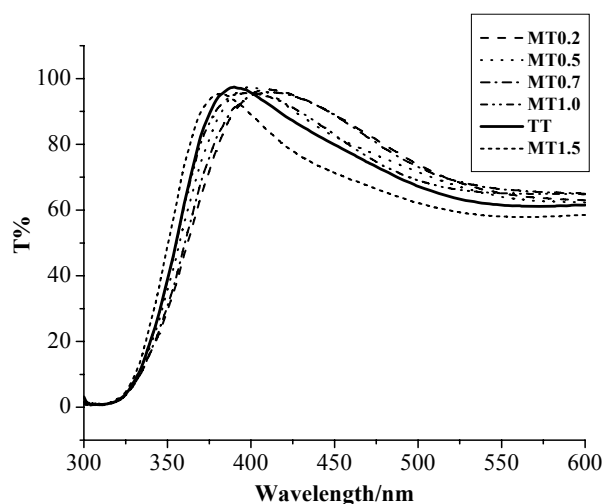


**Fig. 9** The UV-Vis transmittance of the TiO<sub>2</sub> films doped by Mn with different dopant concentration.

Mn ion exists as Mn<sup>4+</sup> after Mn-doped TiO<sub>2</sub> are treated at 500° [13]. The configuration of the extra-nuclear electron of Mn<sup>4+</sup> is 3s<sup>2</sup>3p<sup>6</sup>3d<sup>3</sup>, which lean to return to that of 3s<sup>2</sup>3p<sup>6</sup>3d<sup>5</sup> (Mn<sup>2+</sup>), which is stably-associated with the half-filled subshells (3d<sup>5</sup>). With UV radiation, there are photon-generated carriers within the semiconductor. The Mn<sup>4+</sup> in the bottom layer becomes the electron acceptor, and the photon-generated electrons transfer from surface layer to bottom layer in the films. Thus the PN junction might be established in the doped TiO<sub>2</sub> film with N-type fields in the bottom layer and P-type fields in the surface layer. When diffusion of the carriers reaches equilibrium, each Fermi level in the system is at the same level, but the band near to the interface bends and forms a potential barrier of current carriers, namely, a space-charge region [15]. In our proceeding paper [8], we proved the existence of PN junction in the films and its importance to the

separation of photon-generated carriers. The P-N junction becomes the effective trap to capture excitation electron and restrict the recombination of photo-generated electron-hole pairs, and photo-generated current carriers are separated which is exhibited as the strong photocurrent. Then there are the holes enrichment in the surface layer leaning to react with organic or H<sub>2</sub>O adsorbed on the surface. So the photocatalytic activity is enhanced. The sketch map is shown in Fig. 10. However, the structure of PN junction would be greatly affected by the Mn doping concentration.

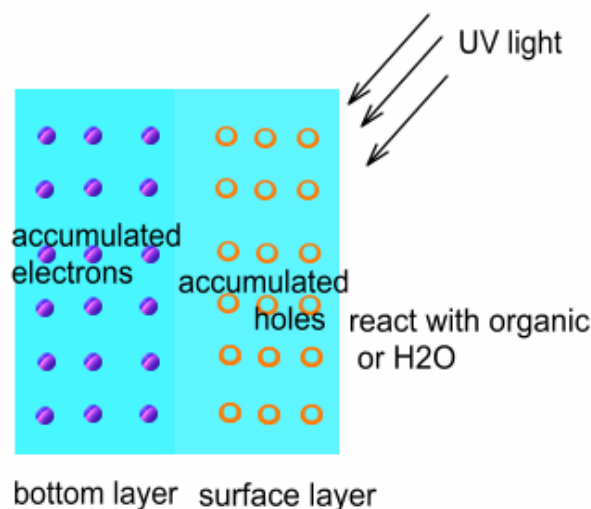


**Fig. 10** The sketch map of the photo-generated carriers' separation in the bottom layer doped TiO<sub>2</sub> film

When Mn doping concentration in the bottom layer is low, the depletion layer can not form, and then photo-generated carriers can not be separated effectively.

When the dopant of Mn ions in the bottom layer is in a certain concentration range, linearly-graded junction would form inside the films under the cooperation of drive-in diffusion and field-aided diffusion [16]. The space-charge region of the linearly-graded junction, act as a rapid separation site for the photogenerated electrons and holes, holding back the recombination of electrons and holes with increasing the lifetime of current carriers, thus open circuit potential and photocurrent intensify. Upon UV excitation, photogenerated electrons accumulate at the bottom layer, whereas holes could accumulate at the surface layer. Accumulation of holes at the surface layer led to the production of surface hydroxyl radical  $\cdot\text{OH}$ , which was responsible for the oxidation decomposition of methyl orange. As for the Mn doping TiO<sub>2</sub> Film at bottom layer, photogenerated electrons were effectively accumulated to bottom layer without recombining with holes. This led to the significant enhancement of the photocatalytic activity of the thin films. Many research works [17, 18] showed that the composite of two kinds of semiconductors or two phases of the same semiconductor was beneficial in reducing the recombination of photogenerated electrons and holes and thus enhanced photocatalytic activity.

In the films, photon-generated carrier separation is affected by the space-charge region, which is a function of dopant concentration gradient. Because the more dopant in the

bottom layer (such as 1.0 at % and 1.5 at %) could decrease concentration gradient of dopant due to the diffusion in process of heat treatment, there would be a maximal width of space-charge region along with an optimal dopant concentration. So there exists an optimal dopant concentration (0.7 at %) in MT film.

For the MM films, where Mn was uniformly doped in the TiO<sub>2</sub> thin films, PN junction in the semiconductor can not be constructed. On the contrary, Mn in TiO<sub>2</sub> film shortens the distance of recombination of electron-hole pairs, so the photocatalytic activity decreases.

## 5 Conclusions

The thin films of TiO<sub>2</sub> doped by Mn with different dopant concentration are prepared by sol-gel method under process control. Mn non-uniformly doping can evidently enhance the photocatalytic activity of the TiO<sub>2</sub> films, and there was an optimal dopant concentration of 0.7 at %, whereas Mn uniformly doping has a detrimental effect on its photoactivity. For the Mn non-uniformly doping TiO<sub>2</sub> film, the effect of dopant concentration on the photocatalytic activity, spectral shift and photo-electrochemical properties can be explained based on the establishing of PN junction in the semiconductor to induce the separation of photo-generated carriers.

## Acknowledgment

The authors are grateful for financial support from Guangdong Natural Science Foundation (Project No.32708).

## References

- [1] M.R. Hoffmann, S.T. Martin, W. Choi and D.W. Bahnemann: "Environmental applications of semiconductor photocatalysis", *Chem. Rev.*, Vol. 95, (1995), pp. 69–72.
- [2] Y.M. Cho, W.Y. Choi, C.H. Lee, T. Hyeon and H.I. Lee: "Visible light-induced degradation of carbon tetrachloride on dye-sensitized TiO<sub>2</sub>", *Environ. Sci. Technol.*, Vol. 35, (2001), pp. 966–970.
- [3] W. Choi, J.Y. Ko, H. Park and J.S. Chung: "Investigation on TiO<sub>2</sub>-coated optical fibers for gas-phase photocatalytic oxidation of acetone", *Appl. Catal. B: Environ.*, Vol. 31, (2001), pp. 209–213.
- [4] W.Y. Teoh, L. Madler, D. Beydoun, S.E. Pratsinis and R. Amal: "Direct (one-step) synthesis of TiO<sub>2</sub> and Pt/TiO<sub>2</sub> nanoparticles for photocatalytic mineralisation of sucrose", *Chem. Eng. Sci.*, Vol. 60, (2005), pp. 5852–5861.
- [5] M. Hirano and K. Ota: "Direct formation and photocatalytic performance of anatase (TiO<sub>2</sub>)/silica (SiO<sub>2</sub>) composite nanoparticles", *J. Am. Ceram. Soc.*, Vol. 87, (2004), pp. 1567–1570.

- [6] A. Di Paola, E. Garcia-Lopez, S. Ikeda, G. Marci, B. Ohtani and L. Palmisano: “Photocatalytic degradation of organic compounds in aqueous systems by transition metal doped polycrystalline  $\text{TiO}_2$ ”, *Catal. Today*, Vol. 75, (2002), pp. 87–93.
- [7] W.Y. Choi, A. Termin and M.R. Hoffmann: “The role of metal-ion dopants in quantum-sized  $\text{TiO}_2$  - correlation between photoreactivity and charge-carrier recombination dynamics”, *J. Phys. Chem.*, Vol. 98, (1994), pp. 13669–13679.
- [8] W. Xu, X.J. Li, S.J. Zheng and J.G. Wang: “Mechanism for Enhanced Photocatalytic Activity of Titanium Dioxide Film Doped by Mn under Control”, *Chem. J. Chinese U.*, Vol. 26, (2005), pp. 2297–2301.
- [9] J.G. Yu and X.J. Zhao: “Effect of surface treatment on the photocatalytic activity and hydrophilic property of the sol-gel derived  $\text{TiO}_2$  thin films”, *Mater. Res. Bull.*, Vol. 36, (2001), pp. 97–107.
- [10] J.G. Yu and X.J. Zhao: “Preparation and microstructure of the porous  $\text{TiO}_2$  nanometer thin films by sol-gel method”, *J. Inorg. Mater.*, Vol. 15, (2000), pp. 347–355.
- [11] Y. Yang, X.J. Li, J.T. Chen and L.Y. Wang: “Effect of doping mode on the photocatalytic activities of  $\text{Mo/TiO}_2$ ”, *J. Photochem. Photobiol. A: Chemistry*, Vol. 163, (2004), pp. 517–522.
- [12] Y. Zhang, J.C. Crittenden, D.W. Hand and D.L. Perram: “Fixed-bed photocatalysts for solar decontamination of water”, *Environ. Sci. Technol.*, Vol. 28, (1994), pp. 435–442.
- [13] S.W. Ding, L.Y. Wang, S.Y. Zhang, Q.X. Zhou, Y. Ding, S.J. Liu, Y.C. Liu and Q.Y. Kang: “Hydrothermal synthesis, structure and photocatalytic property of nano- $\text{TiO}_2\text{-MnO}_2$ ”, *Sci. China. Ser. B*, Vol. 46, (2003), pp. 542–548.
- [14] W.D. Kingery, H.K. Bowen and D.R. Uhlmann (Eds.): *Introduction to Ceramics*, 2nd ed., John Wiley & Sons, New York, 1976.
- [15] Y.Q. Wang, H.M. Cheng and J.M. Ma: “The photoelectrochemical properties of composite titanium dioxide and ferric oxide nanocrystalline electrodes”, *Acta Phys.-Chem. Sin.*, Vol. 15, (1999), pp. 222–227.
- [16] A.S. Grove (Ed.): *Physics and Technology of Semiconductor Devices*, John Wiley & Sons, New York, 1976.
- [17] J.G. Yu, J.F. Xiong, B. Cheng and S.W. Liu: “Fabrication and characterization of  $\text{Ag-TiO}_2$  multiphase nanocomposite thin films with enhanced photocatalytic activity”, *Appl. Catal. B: Environ.*, Vol. 60, (2005), pp. 211–221.
- [18] T. Kawahara, Y. Konishi, H. Tada, N. Tohge, J. Nishii and S. Ito: “A patterned  $\text{TiO}_2$ (Anatase)/ $\text{TiO}_2$ (Rutile) bilayer-type photocatalyst: Effect of the Anatase/Rutile junction on the photocatalytic activity”, *Angew. Chem. Int. Ed.*, Vol. 41, (2002), pp. 2811–2813.